Roughness-induced piezoelectric scattering in lattice-mismatched semiconductor quantum wells

Doan Nhat Quang
Department of Physics, Graduate School of Science, Osaka University, 1-1 Machikaneyama, Toyonaka, Osaka 560-0043, Japan

Vu Ngoc Tuoc
FB 6-Theoretische Physik, Universität Paderborn, Warburger 100, 33098 Paderborn, Germany

Tran Doan Huan
Institute of Engineering Physics, Hanoi University of Technology, 1 Dai Co Viet Road, Hanoi, Vietnam
(Received 26 June 2002; revised manuscript received 21 August 2003; published 21 November 2003)

We present a theory of the mobility of electrons in real semiconductor quantum wells (QW's) made from lattice-mismatched epitaxial layers. In the case of zinc-blende structure QW's, we prove that besides the conventional scattering mechanisms, e.g., impurity doping, surface roughness, and alloy disorder there exists an *ad hoc* scattering source, which is due to a large fluctuating density of roughness-induced piezoelectric charges. Scattering by their piezoelectric field is found to be a new important scattering mechanism limiting the electron mobility of real strained QW's, especially those with a well thickness of the order of or greater than 50 Å. By incorporating this scattering into the theory, we are able to provide a perfect explanation for the low-temperature electron mobility measured in lattice-mismatched InGaAs-based QW's, which has not been understood starting from the so far-known scattering sources. The possibility of applying our theory to other lattice-mismatched systems such as Si/SiGe heterostructures and nitride-based QW's is outlined.

DOI: 10.1103/PhysRevB.68.195316 PACS number(s): 73.50.Bk, 73.63.Hs, 77.65.Ly

I. INTRODUCTION

It is well known[1] that transport properties of a two-dimensional electron gas (2DEG) in a semiconductor quantum well (QW) can be strongly affected by the quality of interfaces between the well and barrier layers. The QW can be in an unstrained or strained status in dependence on lattice match or mismatch of the well layer to the barriers. For any (unstrained or strained) QW, interface roughness was shown[2] to produce random fluctuations in the well width, which modulate the confinement energy and result in a scattering potential for the 2D motion of confined charge carriers. Hereafter, this conventional treatment of interface roughness is, for short, referred to as surface roughness scattering and has been considered by a number of authors.[2–5]

It was pointed out that in combination with other scattering sources, viz. impurity doping and alloy disorder, surface roughness scattering is able to quantitatively describe experimental findings about the low-temperature mobility of electrons in lattice-matched QW's, e.g., made from GaAs/AlAs (Ref. 4). Nevertheless, it has been shown that the well-known scattering mechanisms turn out to fail in the interpretation of the electron mobility measured in some lattice-mismatched QW's, e.g., from $In_{0.2}Ga_{0.8}As/GaAs$ (Ref. 6) and $In_{0.15}Ga_{0.85}As/Al_{0.23}Ga_{0.77}As$ (Ref. 7). Therefore, Lyo and Fritz[6] had to assume another source of scattering which stems from strain fluctuations due to a random distribution of In atoms. However, their theory was found to be unable to explain a large difference in the mobility of the samples studied in Refs. 6 and 7, in which the difference in the structure and the In content is small. So far, this has remained as a challenging problem in the theory of electron mobility for lattice-mismatched InGaAs-based QW's. On the other hand, a full understanding of scattering mechanisms in these systems is clearly of great interest since they have been extensively applied in electronic and optoelectronic devices.

It was indicated[8–11] that interface roughness gives rise to drastic fluctuations in a strain field. As a result, Feenstra and Lutz[9] found that for Si/SiGe heterostructures, the roughness-induced strain variations cause a random shift of the conduction band edge. This, in turn, generates a perturbing deformation potential as a new scattering source, which yields much better agreement with experimental data[12] than surface roughness scattering does.

Recently, Quang and co-workers[10,11] have proved that due to interface roughness the strain field in a well layer of cubic symmetry has nonvanishing shear components even if it has been grown on a [001]-oriented substrate. Therefore, in an actual strained zinc-blende structure QW there exists a large fluctuating density of bound piezoelectric charges and a high relevant electric field. The random piezoelectric field must also act as a scattering mechanism. In what follows, this is simply referred to as piezoelectric scattering (not confused with that due to acoustic phonons) and, to date, has not been considered within the area of transport theory.

Thus, the goal of our paper is to develop a theory of the low-temperature mobility of charge carriers in *real lattice-mismatched* QW's, taking explicitly into the roughness-induced piezoelectric field. We will be concerned mainly with QW's made of zinc-blende structure material, e.g., InGaAs, especially grown on a (001) substrate. However, we will give a brief discussion on the possibility of applying our theory to describe transport in other lattice-mismatched systems such as Si/SiGe heterostructures and nitride-based QW's.

The paper is organized as follows. In Sec. II below, we formulate our model and the basic equations used to calculate the low-temperature disorder-limited 2DEG mobility in

terms of an autocorrelation function. This function is derived in Sec. III for surface roughness scattering in a square QW, taking adequate account of the finiteness of its potential barriers. In Sec. IV, this function is derived for piezoelectric scattering which appears as an effect due to both lattice mismatch and interface roughness, taking plausible account of elastic anisotropy of cubic crystals. Section V is devoted to numerical results, conclusions, and application of the theory to explain some experimental findings. Finally, a summary is presented in Sec. VI.

II. BASIC FORMULATION

A. Finitely deep square quantum well

In plenty of semiconductor heterostructures of physical interest, disorder is usually caused by some random field associated, e.g., with impurity doping, surface roughness, and alloying.[1,3–5] Hereafter, we restrict the discussion to the case when the random field $U(\mathbf{r},z)$ is Gaussian and it may be therefore completely characterized by an autocorrelation function. The random field is conveniently handled by a 2D Fourier expansion:

$$U(\mathbf{r},z)=\sum_{\mathbf{q}} U(\mathbf{q},z)e^{i\mathbf{q}\cdot\mathbf{r}}, \tag{1}$$

where $\mathbf{r}=(x,y)$ represents a 2D position vector in the plane of the 2DEG, and z the growth direction, e.g., [001].

In order to allow for the finite extension of electron states along the growth direction, the disorder potential is to be averaged with the envelope wave function of a 2D subband:

$$U(\mathbf{q})=\int_{-\infty}^{+\infty} dz|\zeta(z)|^2 U(\mathbf{q},z). \tag{2}$$

The random field is normally assumed to be macroscopically homogeneous in the 2DEG plane. Its autocorrelation function in wave vector space is then given by $\langle|U(\mathbf{q})|^2\rangle$, where the angular brackets stand for averaging over all configurations of the randomness.

It has been pointed out[13–18] that the height of the potential barrier in a semiconductor heterostructure may play an important role in certain phenomena. In particular, the simplifying assumption of infinitely deep wells turns out to considerably overestimate surface roughness scattering, so that the theory cannot explain some experimental data.[15,16] In the case of $In_xGa_{1-x}As/GaAs$ and $In_xGa_{1-x}As/Al_xGa_{1-x}As$ QW's which we will be dealing with, the barrier height is rather small (on the order of 0.1 eV). Therefore, we must, in general, start from the realistic model of finitely deep wells.

At very low temperature the electrons are assumed to primarily occupy the lowest conduction subband. For a square QW, the corresponding exact envelope wave function is provided by

$$\zeta(z)=C\sqrt{\frac{2}{L}}\begin{cases}\cos\left(\frac{1}{2}kL\right)\exp(\kappa z) & \text{for } z<0,\\ \cos\left[k\left(z-\frac{1}{2}L\right)\right] & \text{for } 0\leqslant z\leqslant L,\\ \cos\left(\frac{1}{2}kL\right)\exp[-\kappa(z-L)] & \text{for } z>L.\end{cases} \tag{3}$$

Here C is a normalization constant determined by

$$C^2\left(1+\frac{\sin a}{a}+\frac{1+\cos a}{b}\right)=1, \tag{4}$$

in which $a=kL$ and $b=\kappa L$ are dimensionless wave numbers in the well and the barriers. These are fixed by both the well thickness L and the barrier height V_0 as follows:

$$a=\frac{L\sqrt{2m_zV_0}}{\hbar}\cos\left(\frac{1}{2}a\right) \tag{5}$$

and

$$b=a\tan\left(\frac{1}{2}a\right), \tag{6}$$

with m_z as an effective mass of the charge carriers along the growth direction.

B. Low-temperature electron mobility

At zero temperature the mobility is determined via the momentum relaxation time τ by a simple relation

$$\mu=e\tau/m^*, \tag{7}$$

where we assume a parabolic subband with an effective mass of the charge carriers m^*. A general expression for the relaxation time of a d-dimensional electron gas subjected to a disorder was derived by Gold and Götze[19] within a multiple scattering theory. In what follows, for simplicity, we will ignore the multiple scattering effects.

Within the linear transport theory, the inverse relaxation time for zero temperature is expressed in terms of the autocorrelation function of disorder:[20,21]

$$\frac{1}{\tau}=\frac{1}{(2\pi)^2\hbar E_F}\int_0^{2k_F}dq\int_0^{2\pi}d\theta\frac{q^2}{(4k_F^2-q^2)^{1/2}}\frac{\langle|U(\mathbf{q})|^2\rangle}{\varepsilon^2(q)}, \tag{8}$$

where $\mathbf{q}=(q,\theta)$ means a 2D wave vector in the x-y plane given in terms of polar coordinates, $E_F=\hbar^2k_F^2/2m^*$ is the Fermi energy, and k_F the Fermi wave number fixed by the sheet electron density: $k_F=\sqrt{2\pi n_s}$. The angle integral appears in Eq. (8) since the autocorrelation function of a random field may have a directional dependence as seen in Eq. (46) below.

The dielectric function $\varepsilon(q)$ in Eq. (8) allows for the screening of a scattering potential by the 2DEG. There are a

number of possible choices for this function. Within the random phase approximation, this is supplied at zero temperature by[1]

$$\varepsilon(q)=1+\frac{q_{\mathrm{TF}}}{q}C^4F_{\mathrm{S}}(qL)[1-G(q)] \quad \text{for } q\leqslant 2k_{\mathrm{F}}, \tag{9}$$

with C as the normalization constant from Eq. (4). The inverse 2D Thomas-Fermi screening length is given by

$$q_{\mathrm{TF}}=\frac{2m^*e^2}{\varepsilon_{\mathrm{L}}\hbar^2}, \tag{10}$$

where ε_{L} is the dielectric constant of the system, neglecting a small difference in its values for the well and the barriers.

The screening form factor $F_{\mathrm{S}}(qL)$ figuring in Eq. (9) accounts for the extension of electron states along the growth direction, defined by

$$F_{\mathrm{S}}(qL)=\frac{1}{C^4}\int_{-\infty}^{+\infty}dz\int_{-\infty}^{+\infty}dz'|\zeta(z)|^2\,|\zeta(z')|^2\,e^{-q|z-z'|}. \tag{11}$$

By means of Eq. (3) for the lowest subband, this may be written in terms of a function of the dimensionless variable $t=qL$, given by

$$F_{\mathrm{S}}(t)=s_1(t)+s_2(t)+s_3(t), \tag{12}$$

where by definition:

$$s_1(t)=\frac{2}{t}\left(1+\frac{\sin a}{a}\right)+\frac{t}{t^2+4a^2}\left(1+2\frac{\sin a}{a}+\frac{\sin 2a}{2a}\right)$$
$$-4e^{-t/2}\left(\frac{1}{t}-\frac{2a\sin a-t\cos a}{t^2+4a^2}\right)\left[\frac{2a\sin a}{t^2+4a^2}\cosh\left(\frac{1}{2}t\right)\right.$$
$$\left.+\left(\frac{1}{t}+\frac{t\cos a}{t^2+4a^2}\right)\sinh\left(\frac{1}{2}t\right)\right], \tag{13}$$

$$s_2(t)=8(1+\cos a)\frac{e^{-t/2}}{t+2b}\left[\frac{2a\sin a}{t^2+4a^2}\cosh\left(\frac{1}{2}t\right)\right.$$
$$\left.+\left(\frac{1}{t}+\frac{t\cos a}{t^2+4a^2}\right)\sinh\left(\frac{1}{2}t\right)\right], \tag{14}$$

and

$$s_3(t)=2(1+\cos a)^2\left[\frac{e^{-t}}{(t+2b)^2}+\frac{t-2b}{2b(t^2-4b^2)}\right], \tag{15}$$

with a and b as the dimensionless wave numbers from Eqs. (5) and (6), respectively.

In the limiting case of $V_0\to\infty$, we have $C=1$ and $a=\pi$, so that Eqs. (12)–(15) reproduce the well-known formula for the screening form factor for infinitely deep wells.[22]

Finally, the function $G(q)$ appears in Eq. (9) to include the local field corrections connected with the many-body interaction in the 2DEG. Within Hubbard's approximation, in which merely the exchange effect is involved, it holds[23]

$$G(q)=\frac{q}{2(q^2+k_{\mathrm{F}}^2)^{1/2}}. \tag{16}$$

In the case when the 2DEG experiences simultaneously several sources of scattering, viz. surface roughness and piezoelectric, the total relaxation time is determined by

$$\frac{1}{\tau_{\mathrm{tot}}}=\frac{2}{\tau_{\mathrm{SR}}}+\frac{2}{\tau_{\mathrm{PE}}}, \tag{17}$$

in which we have introduced a factor of 2 on the right-hand side to include the effects from both interfaces of the QW.

III. SURFACE ROUGHNESS SCATTERING

As clearly seen from Eq. (8), in the calculation of the mobility limited by each scattering mechanism, we need to specify its autocorrelation function $\langle|U(\mathbf{q})|^2\rangle$. This implies that we ought to evaluate the Fourier transform of the scattering potential averaged with the envelope wave function of the lowest 2D subband.

First, we treat scattering of confined charge carriers from a rough potential barrier of a finite height V_0. The scattering potential is due to fluctuations in the position of the barrier, so that[1]

$$U_{\mathrm{SR}}(\mathbf{r},z)=V_0\Delta(\mathbf{r})\,\delta(z). \tag{18}$$

Then, the average scattering potential in wave vector space is determined by the value of an envelope wave function at the barrier plane $z=0$ as follows:

$$U_{\mathrm{SR}}(\mathbf{q})=V_0|\zeta(0)|^2\Delta_{\mathbf{q}}, \tag{19}$$

where $\Delta_{\mathbf{q}}$ is a Fourier transform of the interface profile. By means of Eq. (3) for the lowest subband, this reads

$$U_{\mathrm{SR}}(\mathbf{q})=\frac{\hbar^2C^2a^2}{m_zL^3}\Delta_{\mathbf{q}}, \tag{20}$$

with C, a, and L, as before, the normalization constant, the dimensionless wave number in the well, and its thickness, respectively.

Thus, the autocorrelation function of interest depends on the spectral distribution of the interface profile. For simplicity, this is normally chosen in a Gaussian form[1]

$$\langle|\Delta_{\mathbf{q}}|^2\rangle=\pi\Delta^2\Lambda^2\exp(-q^2\Lambda^2/4), \tag{21}$$

where Δ and Λ are a roughness amplitude and correlation length, respectively.

For conventional surface roughness scattering from an arbitrarily high barrier, we may obtain the autocorrelation function in a simple analytic form:

$$\langle|U_{\mathrm{SR}}(\mathbf{q})|^2\rangle=\left(\frac{\pi^{1/2}\hbar^2C^2a^2\Delta\Lambda}{m_zL^3}\right)^2\exp(-q^2\Lambda^2/4). \tag{22}$$

In the limiting case of $V_0 \to \infty$: $C=1$ and $a=\pi$, this reproduces the well-known L^6-dependence of the mobility governed by surface roughness scattering in infinitely deep wells.[3,5,21] In the opposite case: $C=a/2$ with $a=L\sqrt{2m_z V_0/\hbar}$, this reproduces the L^2-dependence for ultrathin wells.[15,16]

It is to be noted that in the previous calculations[6,15,16] the average scattering potential was supposed to be equal to spatial fluctuations in the confinement energy due to roughness-induced changes in the well thickness. Then, an analytic expression for the autocorrelation function is obtained merely in the two above limiting cases.

IV. ROUGHNESS-INDUCED PIEZOELECTRIC SCATTERING

A. Strain fluctuations

We now turn to scattering related to piezoelectricity of the well material. Let us examine a QW made from a strained layer sandwiched between two unstrained layers, in which the well thickness is small but the barrier ones are large compared with the critical thickness. The lattice mismatch is defined in terms of the lattice constants of the well and barrier by

$$\epsilon_{\parallel}=\frac{a_{\mathrm{b}}-a_{\mathrm{w}}}{a_{\mathrm{w}}}. \tag{23}$$

It is well known[24,25] that if the well layer is of cubic symmetry, the substrate has been oriented along a high symmetry direction, e.g., [001], and the interfaces between the well and barriers are assumed to be ideal, i.e., absolutely flat; the stress field inside of the well is uniform and biaxial. In what follows, the crystal reference system is, as usual, such that the z axis coincides with the [001] growth direction. The stress field is then supplied by

$$\sigma_{\mathrm{F}}=[\sigma,\sigma,0,0,0,0], \quad \sigma=\frac{1}{2}G\epsilon_{\parallel}. \tag{24}$$

Accordingly, the strain field within the well is also uniform and has vanishing off-diagonal components, given by

$$\epsilon_{\mathrm{F}}=[\epsilon_{\parallel},\epsilon_{\parallel},\epsilon_{\perp},0,0,0], \quad \epsilon_{\perp}=-K\epsilon_{\parallel}. \tag{25}$$

Here, the elastic constants of the strained layer are defined by[26]

$$K=2\frac{c_{12}}{c_{11}}, \quad G=2(K+1)(c_{11}-c_{12}), \tag{26}$$

with c_{11}, c_{12}, and c_{44} as its elastic stiffness constants.

It should be emphasized[27,28] that actual semiconductor heterostructures always exhibit lateral feature in the form of interface roughness. The roughening of an interface, which imposes a boundary condition for elastic lattice deformation in the well, is demonstrated[8,9] to result in drastic fluctuations of the stress and strain fields. On the other hand, the roughness forms during growth as an important mechanism for strain relaxation. Indeed, a fraction of the elastic strain energy in the well is transmitted via interfaces into the unstrained barriers, thus lowering the total energy of the well and its strain fluctuations. The effect from a rough buried (barrier/well) interface on the stress field was derived by Feenstra and Lutz,[9] assuming that the system is of elastic isotropy.

Unfortunately, the elastic properties of almost all cubic crystals of interest are significantly anisotropic. It is well known[29] that the deviation of cubic symmetry from isotropy is measured by an anisotropy ratio:

$$A=2\frac{c_{44}}{c_{11}-c_{12}}, \tag{27}$$

which is generally somewhat large, e.g., $A=1.83$ and 2.79 for GaAs and InAs, respectively. It has been indicated[30–33] that the isotropic approximation cannot precisely describe these materials. Therefore, in the literature several improvements have been made for various low-dimensional semiconductor heterostructures.[32,33]

Recently, it has been experimentally shown[30] that the assumption of elastic isotropy remarkably overestimated strain relaxation, so that this could give only a lower bound for the values of strain in the well. Furthermore, in the case of misfit dislocation-induced relaxation the ratio of the measured strain to this lower bound was found to likely be of the order of the anisotropy ratio. Therefore, one should incorporate the reduction of roughness-induced relaxation arising from elastic anisotropy into the theory of Feenstra and Lutz.[9] We will assume that this reduction of strain relaxation gives rise to an enhancement of strain fluctuations by a factor equal to the anisotropy ratio. Consequently, the effect from a rough buried interface located at $z=0$ on the status of stress inside of the well is plausibly described by a 2D Fourier expansion for the stress field as follows:

$$\begin{aligned}
\sigma_{xx}(\mathbf{r},z)&=\sigma+\frac{A\sigma}{2}\sum_{\mathbf{q}} q\Delta_{\mathbf{q}}e^{-qz}\cos^2\theta e^{i\mathbf{q}\cdot\mathbf{r}},\\
\sigma_{yy}(\mathbf{r},z)&=\sigma+\frac{A\sigma}{2}\sum_{\mathbf{q}} q\Delta_{\mathbf{q}}e^{-qz}\sin^2\theta e^{i\mathbf{q}\cdot\mathbf{r}},\\
\sigma_{zz}(\mathbf{r},z)&=-\frac{A\sigma}{2}\sum_{\mathbf{q}} q\Delta_{\mathbf{q}}e^{-qz}e^{i\mathbf{q}\cdot\mathbf{r}},\\
\sigma_{yz}(\mathbf{r},z)&=\frac{A\sigma}{2}\sum_{\mathbf{q}} q\Delta_{\mathbf{q}}e^{-qz}\sin\theta e^{i(\mathbf{q}\cdot\mathbf{r}+\pi/2)},\\
\sigma_{zx}(\mathbf{r},z)&=\frac{A\sigma}{2}\sum_{\mathbf{q}} q\Delta_{\mathbf{q}}e^{-qz}\cos\theta e^{i(\mathbf{q}\cdot\mathbf{r}+\pi/2)},\\
\sigma_{xy}(\mathbf{r},z)&=\frac{A\sigma}{4}\sum_{\mathbf{q}} q\Delta_{\mathbf{q}}e^{-qz}\sin 2\theta e^{i\mathbf{q}\cdot\mathbf{r}},
\end{aligned} \tag{28}$$

where $0\leqslant z\leqslant L$, and $\Delta_{\mathbf{q}}$ is as before a Fourier transform of the interface profile with $\mathbf{q}=(q,\theta)$, as a 2D wave vector given in polar coordinates. It is to be noted that in difference

from the earlier theories,[8–11] we have included elastic anisotropy of the well layer in terms of an anisotropy factor $A>1$.

With the use of Hooke's law,[24,34] the strain field within the well is readily determined from Eq. (28) to be

$$\begin{aligned}
\epsilon_{xx}(\mathbf{r},z)&=\epsilon_{\parallel}+\frac{(K+1)A\epsilon_{\parallel}}{2}\sum_{\mathbf{q}} q\Delta_{\mathbf{q}}e^{-qz}\cos^2\theta e^{i\mathbf{q}\cdot\mathbf{r}},\\
\epsilon_{yy}(\mathbf{r},z)&=\epsilon_{\parallel}+\frac{(K+1)A\epsilon_{\parallel}}{2}\sum_{\mathbf{q}} q\Delta_{\mathbf{q}}e^{-qz}\sin^2\theta e^{i\mathbf{q}\cdot\mathbf{r}},\\
\epsilon_{zz}(\mathbf{r},z)&=\epsilon_{\perp}-\frac{(K+1)A\epsilon_{\parallel}}{2}\sum_{\mathbf{q}} q\Delta_{\mathbf{q}}e^{-qz}e^{i\mathbf{q}\cdot\mathbf{r}},\\
\epsilon_{yz}(\mathbf{r},z)&=\frac{GA\epsilon_{\parallel}}{8c_{44}}\sum_{\mathbf{q}} q\Delta_{\mathbf{q}}e^{-qz}\sin\theta e^{i(\mathbf{q}\cdot\mathbf{r}+\pi/2)},\\
\epsilon_{zx}(\mathbf{r},z)&=\frac{GA\epsilon_{\parallel}}{8c_{44}}\sum_{\mathbf{q}} q\Delta_{\mathbf{q}}e^{-qz}\cos\theta e^{i(\mathbf{q}\cdot\mathbf{r}+\pi/2)},\\
\epsilon_{xy}(\mathbf{r},z)&=\frac{GA\epsilon_{\parallel}}{16c_{44}}\sum_{\mathbf{q}} q\Delta_{\mathbf{q}}e^{-qz}\sin 2\theta e^{i\mathbf{q}\cdot\mathbf{r}}.
\end{aligned}\tag{29}$$

It is obviously seen from Eqs. (28) and (29) that in comparison to the case of ideal interfaces described by Eqs. (24) and (25), the stress and strain fields within the well of a real lattice-mismatched semiconductor QW are fundamentally changed, being random in nature and microscopically nonuniform. Moreover, it is distinctive of the system with a rough interface that the strain field is of both hydrostatic and shear origins, having *nonvanishing* off-diagonal components although grown on a (001) substrate.

B. Piezoelectric charge density

Next, we are dealing with macroscopic properties of a well layer which is made of zinc-blende structure material. The nonzero off-diagonal components of a strain field induce a polarization vector inside of the well:[34,35]

$$P_i=2e_{14}\epsilon_{jk}\quad (i\neq j\neq k),\tag{30}$$

with e_{14} its piezoelectric constant.

So far, it has been demonstrated[25,28,35] that a strained layer which is made of zinc-blende material and grown on a [001]-oriented substrate exhibits neither a piezoelectric polarization nor any piezoelectric field. Nevertheless, it should be emphasized that this conclusion was, in fact, drawn simply for the case of ideal interfaces. All experimentally accessible structures are real semiconductor QW's with rough interfaces and, as quoted above, have nonzero shear strains. Upon inserting ϵ_{jk} $(j\neq k)$ from Eq. (29) into Eq. (30), one may arrive at a 2D Fourier expansion for the piezoelectric polarization

$$\begin{aligned}
P_x(\mathbf{r},z)&=\frac{e_{14}GA\epsilon_{\parallel}}{4c_{44}}\sum_{\mathbf{q}} q\Delta_{\mathbf{q}}e^{-qz}\sin\theta e^{i(\mathbf{q}\cdot\mathbf{r}+\pi/2)},\\
P_y(\mathbf{r},z)&=\frac{e_{14}GA\epsilon_{\parallel}}{4c_{44}}\sum_{\mathbf{q}} q\Delta_{\mathbf{q}}e^{-qz}\cos\theta e^{i(\mathbf{q}\cdot\mathbf{r}+\pi/2)},\\
P_z(\mathbf{r},z)&=\frac{e_{14}GA\epsilon_{\parallel}}{8c_{44}}\sum_{\mathbf{q}} q\Delta_{\mathbf{q}}e^{-qz}\sin 2\theta e^{i\mathbf{q}\cdot\mathbf{r}}.
\end{aligned}\tag{31}$$

Equation (31) reveals that in difference from the previous studies,[27,28] the roughness-induced polarization is strongly nonuniform in space. Therefore, a density of fixed charges is generated within the well according to

$$\rho(\mathbf{r},z)=-\nabla\mathbf{P}(\mathbf{r},z).\tag{32}$$

With the aid of Eq. (31), it holds

$$\rho(\mathbf{r},z)=\frac{3e_{14}GA\epsilon_{\parallel}}{8c_{44}}\sum_{\mathbf{q}} q^2\Delta_{\mathbf{q}}e^{-qz}\sin 2\theta e^{i\mathbf{q}\cdot\mathbf{r}}.\tag{33}$$

It is clearly observed from Eq. (33) that in opposition to the earlier theories,[25,28,35] because of roughness there always exist bound piezoelectric charges in the well layer of an actual lattice-mismatched zinc-blende structure QW even with a (001) substrate. The charges are bulklike and randomly distributed in a region inside of the well and near to the interface plane with a zero average but a nonzero rms density.[10,11]

C. Random piezoelectric potential

The bulk piezoelectric charges create an electric field. The unscreened potential energy $U_{\mathrm{PE}}(\mathbf{r},z)$ of an electron of charge $-e$ in this field is derived as a solution of Poisson's equation:

$$\nabla^2[U_{\mathrm{PE}}(\mathbf{r},z)/-e]=(4\pi/\varepsilon_{\mathrm{L}})\rho(\mathbf{r},z).\tag{34}$$

The screening of an electric field by the 2DEG is, as quoted before, described by the dielectric function $\varepsilon(q)$. The piezoelectric potential energy may be represented in terms of an integral extended over the well layer by

$$U_{\mathrm{PE}}(\mathbf{r},z)=\int d\mathbf{r}'dz'\rho(\mathbf{r}',z')v(\mathbf{r}'-\mathbf{r},z'-z),\tag{35}$$

where $v(\mathbf{r}'-\mathbf{r},z'-z)$ stands for the Green's function of Poisson's equation:

$$v(\mathbf{r}'-\mathbf{r},z'-z)=\frac{-e}{\varepsilon_{\mathrm{L}}[(\mathbf{r}'-\mathbf{r})^2+(z'-z)^2]^{1/2}}.\tag{36}$$

On the substitution of Eqs. (33) and (36) into Eq. (35), and the subsequent use of a 2D Fourier transform of the Coulomb potential[1]

$$\int d\mathbf{r}'\frac{e^{i\mathbf{q}\cdot\mathbf{r}'}}{[(\mathbf{r}'-\mathbf{r})^2+(z'-z)^2]^{1/2}}=\frac{2\pi}{q}e^{-q|z'-z|}e^{i\mathbf{q}\cdot\mathbf{r}},\tag{37}$$

we are able to get the 2D Fourier expansion for the piezoelectric potential as given by Eq. (1) with

$$U_{\mathrm{PE}}(\mathbf{q},z)=-\frac{3\pi e e_{14}GA\epsilon_{\parallel}}{4\varepsilon_{\mathrm{L}}c_{44}}q\Delta_{\mathbf{q}}F_{\mathrm{PE}}(q,z;L)\sin 2\theta, \tag{38}$$

in which the form factor for the piezoelectric field is defined by

$$F_{\mathrm{PE}}(q,z;L)=\int_0^L dz' e^{-q(z'+|z'-z|)}. \tag{39}$$

Equation (38) reveals that the piezoelectric field is random with a zero average but a nonzero rms potential.[10,11]

On a straightforward integration, the form factor is cast into a simple form:

$$F_{\mathrm{PE}}(q,z;L)=\frac{1}{2q}\begin{cases} e^{qz}(1-e^{-2qL}) & \text{for } z<0, \\ e^{-qz}(1+2qz)-e^{-q(2L-z)} & \text{for } 0\leqslant z\leqslant L, \\ 2qLe^{-qz} & \text{for } z>L. \end{cases} \tag{40}$$

D. Autocorrelation function of the piezoelectric field

Upon averaging Eqs. (38) and (40) by means of the lowest-subband envelope wave function from Eq. (3), we arrive at an analytic expression for the weighted piezoelectric potential in wave vector space

$$U_{\mathrm{PE}}(\mathbf{q})=-\frac{3\pi e e_{14}GA\epsilon_{\parallel}C^2}{8\varepsilon_{\mathrm{L}}c_{44}}\Delta_{\mathbf{q}}F_{\mathrm{PE}}(qL)\sin 2\theta, \tag{41}$$

with C, as before, the normalization constant fixed by Eq. (4). Here we have introduced a dimensionless form factor for the piezoelectric field as a function of the dimensionless variable $t=qL$ such that

$$F_{\mathrm{PE}}(t)=p_1(t)+p_2(t)\sin a+p_3(t)\cos a, \tag{42}$$

where by definition:

$$p_1(t)=\frac{1-e^{-2t}+2te^{-t}}{t+2b}+\frac{3+e^{-2t}-2(t+2)e^{-t}}{t}, \tag{43}$$

$$p_2(t)=\frac{2a}{t^2+4a^2}\left[1-e^{-2t}+2te^{-t}+4\frac{t^2(1+e^{-t})}{t^2+4a^2}\right], \tag{44}$$

and

$$p_3(t)=\frac{1-e^{-2t}+2te^{-t}}{t+2b}+\frac{t}{t^2+4a^2}\left[1+e^{-2t}-2(t+1)e^{-t}+2\frac{(t^2-4a^2)(1-e^{-t})}{t^2+4a^2}\right], \tag{45}$$

with a and b the dimensionless wave numbers from Eqs. (5) and (6).

TABLE I. Material parameters used: m^* is the effective mass (m_e), a the lattice constant (Å), c_{ij} the elastic stiffness constants (10^{10} Pa), ε_{L} the dielectric constant, and e_{14} the piezoelectric constant (C/m^2).

Material	m^*	a	c_{11}	c_{12}	c_{44}	ε_{L}	e_{14}
GaAs	0.067	5.64191	11.88	5.38	5.94	13.18	−0.16
InAs	0.024	6.0584	8.0	5.1	4.05	14.55	−0.045
$In_{0.2}Ga_{0.8}As$	0.058	5.72521	11.10	5.32	5.56	13.45	−0.137
$In_{0.15}Ga_{0.85}As$	0.061	5.70438	11.30	5.34	5.66	13.39	−0.143

Thus, for piezoelectric scattering we may obtain the following autocorrelation function:

$$\langle|U_{\mathrm{PE}}(\mathbf{q})|^2\rangle=\left(\frac{3\pi^{3/2}ee_{14}GA\epsilon_{\parallel}C^2\Delta\Lambda}{8\varepsilon_{\mathrm{L}}c_{44}}\right)^2F_{\mathrm{PE}}^2(qL)\times\exp(-q^2\Lambda^2/4)\sin^2 2\theta. \tag{46}$$

An examination of Eqs. (46) and (22) shows the probability for piezoelectric scattering depends quadratically on the lattice mismatch $\epsilon_{\parallel}$ and the roughness amplitude Δ, whereas the one for surface roughness scattering merely on the latter. Moreover, it is interesting to note that in the difference from the so far-known scattering sources due, e.g., to impurity doping, surface roughness, and alloy disorder, the autocorrelation function for piezoelectric scattering depends not only on the magnitude of the wave vector but its polar angle as well. Such a directional relation is characteristic also for piezoelectric coupling due to acoustic phonons in the 3D case of bulk semiconductors.[36]

V. RESULTS AND COMPARISON WITH EXPERIMENT

A. Numerical results and conclusions

To illustrate the theory presented in the preceding sections, we have carried out numerical calculations for lattice-mismatched QW's which are made from $In_xGa_{1-x}As$ grown pseudomorphically on a GaAs or AlGaAs substrate. Such systems have been intensively investigated both theoretically and experimentally. The material parameters in use are listed in Table I, where the values for the binary compounds are taken from Refs. 37 and 38, while those for the ternary ones estimated by the virtual crystal approximation.[39] The effective mass of electrons in the growth direction is taken to be equal to their in-plane one: $m_z=m^*$. The barrier height of QW's for electrons is the conduction band offset, which depends on the In content as $V_0=0.6(1144x-255x^2)$ meV,[40] e.g., $V_0=131$ meV for $x=0.2$.

As an example, we have evaluated the electron mobilities of a QW made from $In_{0.2}Ga_{0.8}As$/GaAs, which are limited by interface roughness via both piezoelectric scattering connected with strain fluctuations, μ_{PE}, and surface roughness scattering associated with well-width fluctuations, μ_{SR}. The roughness amplitude Δ enters into the theory sim-

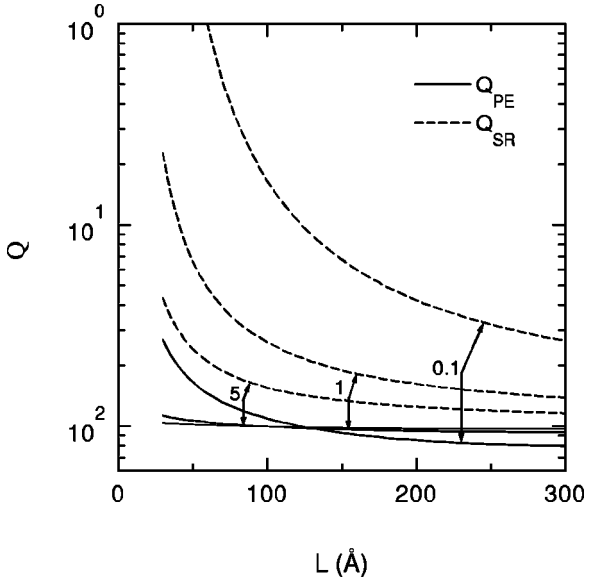

FIG. 1. Ratio $Q=\mu^{\text{fin}}/\mu^{\text{infin}}$ between the electron mobilities for a QW made from $In_{0.2}Ga_{0.8}As/GaAs$, calculated with a finite and an infinite potential barrier vs well width L under a sheet electron density $n_s=10^{12}$ cm^{-2}, a correlation length $\Lambda=50$ Å, and different barrier heights V_0 denoted on lines in units of eV. The solid and dashed lines refer to Q_{PE} and Q_{SR}, respectively.

ply as a scaling factor on which the mobilities exhibit an inverse square dependence, so we may chose some value, say $\Delta=5$ Å.

We now estimate the effect due to the finiteness of the potential barrier height on electron mobilities. This is to be measured by the ratio between the values of the mobility calculated with a finite and an infinite barrier. In the case of surface roughness scattering, the finite-barrier effect on the scattering probability is described by Eq. (22) and is evidently large compared with the one on the dielectric function. For the ratio $Q_{\text{SR}}=\mu_{\text{SR}}^{\text{fin}}/\mu_{\text{SR}}^{\text{infin}}$, we may then immediately obtain as a good approximation:

$$Q_{\text{SR}}=\left(\frac{\pi}{Ca}\right)^4. \tag{47}$$

From this simple relationship and Eqs. (4)–(6), we observe that the finite-barrier effect on the surface roughness-limited mobility, Q_{SR}, shows up in a quite rapid increase when reducing the sizes of the well (depth and thickness) and the effective electron mass along the growth direction. It is interesting to note that this functional dependence on the well depth and that on the effective mass are identical. However, the effect is independent of the surface profile. For piezoelectric scattering, Q_{PE} is dependent on the well sizes, the surface profile as well as the carrier density and the effective mass.

The ratios Q_{SR} and Q_{PE} are depicted in Fig. 1 vs the well thickness L under a correlation length $\Lambda=50$ Å, a sheet electron density $n_s=10^{12}$ cm^{-2}, and different barrier heights $V_0=0.1$, 1, and 5 eV.

The behavior of the calculated mobilities is in detail described in Figs. 2, 3, and 4. Figure 2 displays, according to

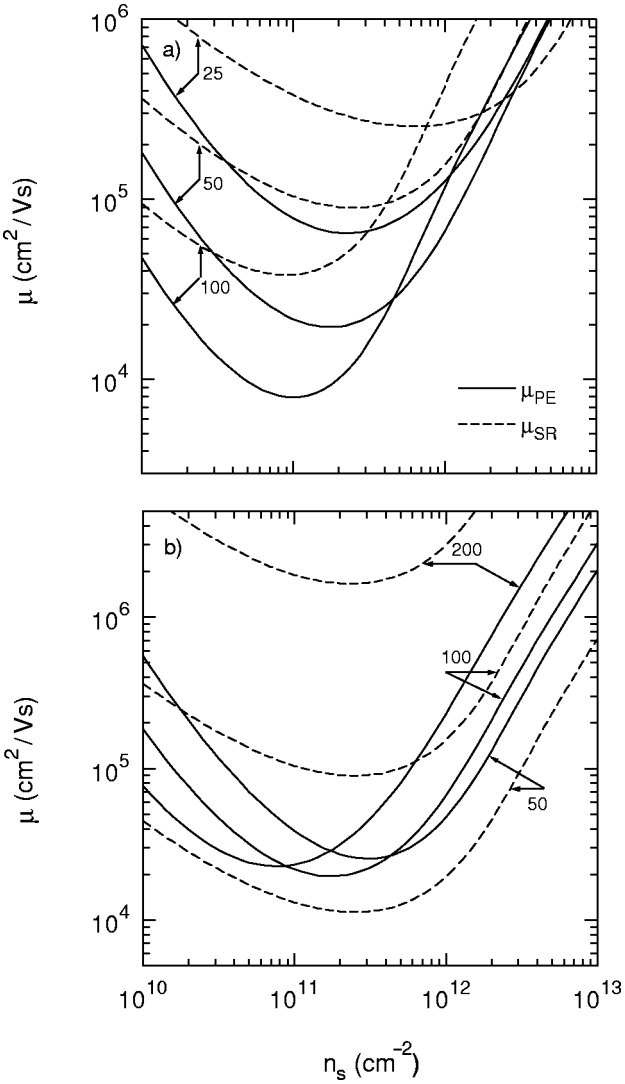

FIG. 2. Mobilities μ_{PE} (solid lines) and μ_{SR} (dashed ones) for the QW in Fig. 1 vs sheet electron density n_s under a roughness amplitude $\Delta=5$ Å and (a) a well width $L=100$ Å and different correlation lengths Λ denoted on lines in units of Å, and (b) a correlation length $\Lambda=50$ Å and various well widths L denoted on lines in units of Å.

Eqs. (7), (8), (22), and (46), the electron mobilities μ_{SR} and μ_{PE} as a function of the sheet carrier density n_s. In Fig. 2(a) this is plotted under a well width $L=100$ Å and different correlation lengths $\Lambda=25$, 50, and 100 Å, whereas in Fig. 2(b) under a correlation length $\Lambda=50$ Å and various well widths $L=50$, 100, and 200 Å. Figure 3 sketches the mobilities against the correlation length Λ. In Fig. 3(a) this is plotted under a carrier density $n_s=10^{12}$ cm^{-2} and different well widths $L=50$, 100, and 200 Å, while in Fig. 3(b) under a well width $L=100$ Å and various carrier densities $n_s=10^{10}$, 10^{11}, and 10^{12} cm^{-2}. Finally, Fig. 4 depicts the mobilities vs the well width L. In Fig. 4(a) this is plotted under a carrier density $n_s=10^{12}$ cm^{-2} and different correlation lengths $\Lambda=50$, 100, and 150 Å, while in Fig. 4(b) under a correlation length $\Lambda=50$ Å and various carrier densities $n_s=10^{10}$, 10^{11}, and 10^{12} cm^{-2}. From the lines thus obtained

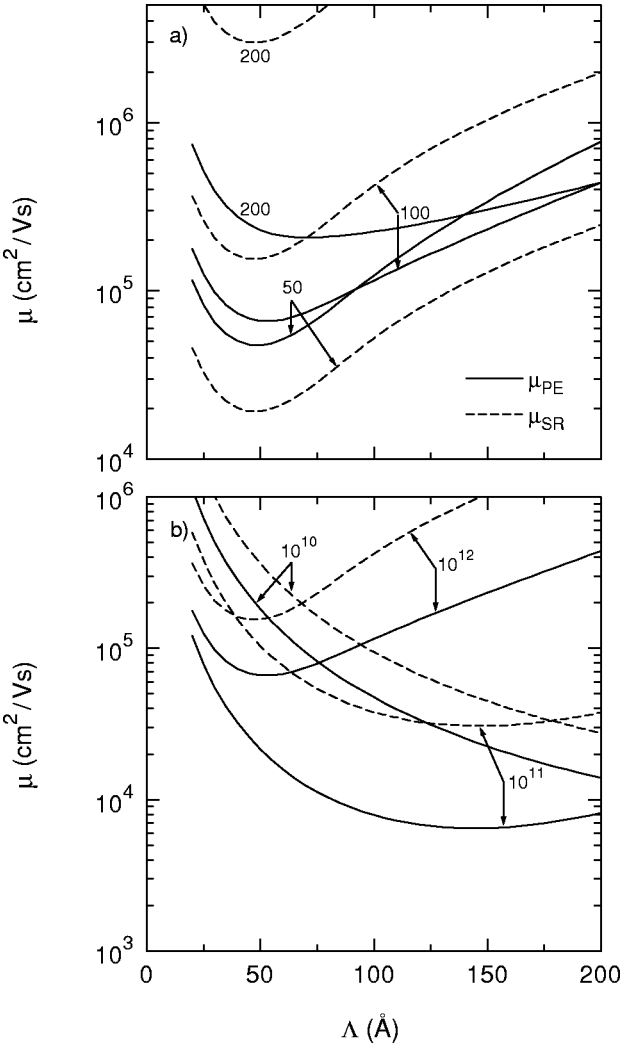

FIG. 3. Mobilities μ_{PE} (solid lines) and μ_{SR} (dashed ones) for the QW in Fig. 1 vs correlation length Λ under a roughness amplitude $\Delta=5$ Å, and (a) an electron density $n_s=10^{12}$ cm^{-2} and different well widths L denoted on lines in units of Å, and (b) a well width $L=100$ Å and various electron densities n_s denoted on lines in units of cm^{-2}.

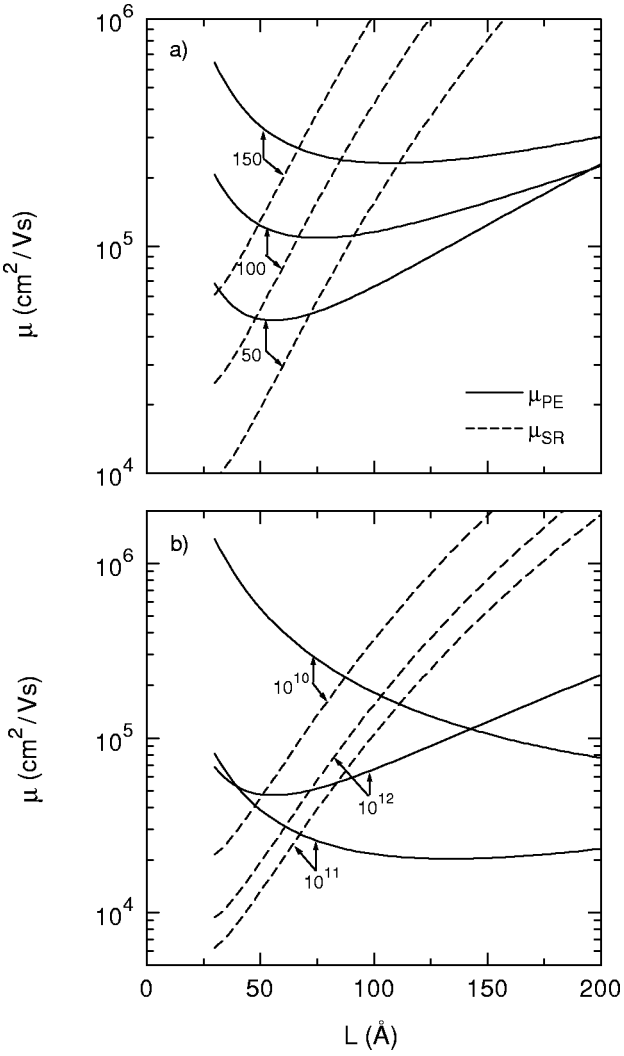

FIG. 4. Mobilities μ_{PE} (solid lines) and μ_{SR} (dashed ones) for the QW in Fig. 1 vs well width L under a roughness amplitude $\Delta=5$ Å and (a) an electron density $n_s=10^{12}$ cm^{-2} and different correlation lengths Λ denoted on lines in units of Å, and (b) a correlation length $\Lambda=50$ Å and various electron densities n_s denoted on lines in units of cm^{-2}.

we may draw the following conclusions.

(i) Figure 1 reveals that the model of infinitely deep wells always overestimates surface roughness scattering: $Q_{SR}>1$. In accordance with the above statement, the finite-barrier effect may become very large for narrow wells, especially under a rather low barrier $V_0<1$ eV and/or a rather thin well $L\lesssim 100$ Å:$Q_{SR}\gg 1$. For instance, $Q_{SR}\sim 17$ under $V_0=0.1$ eV and $L=100$ Å. The effect is found to be significantly larger than that in Si/SiGe QW's,[15,16] since the effective electron mass along the growth direction in $In_xGa_{1-x}AS/GaAS$ QW's is remarkably smaller (by a factor of ~ 16). However, the effect on piezoelectric scattering is not so large: $Q_{PE}\sim 1$. Further, the simplifying model may slightly underestimates this scattering, e.g., under $V_0=0.1$ eV and $L\gtrsim 125$ Å.

(ii) It follows from Fig. 2 that for a fixed correlation length Λ and well width L, the mobilities μ_{PE} and μ_{SR} exhibit similar functions of the electron density n_s. These reach a minimum at some value of n_s. With an increase of Λ and L, the minima are shifted towards lower n_s.

(iii) An inspection of Fig. 3 indicates that the mobilities μ_{PE} and μ_{SR} represent similar functions of the correlation length Λ. These reach a minimum at some value of Λ. In addition, for a wide well: $L\gtrsim 100$ Å, $\mu_{PE}<\mu_{SR}$, i.e., piezoelectric scattering is predominant over surface roughness scattering for all correlation lengths ranging from $\Lambda=25-200$ Å. In contrast, for a narrow well: $L=50$ Å, $\mu_{PE}>\mu_{SR}$.

(iv) Figure 4 shows that with an increase of the well width L the surface roughness-limited mobility μ_{SR} is elevated very rapidly in accordance with Eq. (22), while μ_{PE} exhibits a much weaker dependence on L. The function μ_{PE} reaches a minimum at some value of L, which becomes larger when increasing Λ. In addition, the solid and dashed lines for μ_{PE}

and μ_{SR} belonging to one and the same sample intersect at some L_0 so that for $L<L_0:\mu_{SR}<\mu_{PE}$, and for $L>L_0:\mu_{SR}>\mu_{PE}$. For instance, under $n_s=10^{12}$ cm^{-2} and $\Lambda=50$ Å [Fig. 4(a)]: $L_0=72$ Å, and $\mu_{SR}/\mu_{PE}\sim 2.5$ and 6.5 for $L=100$ and 150 Å, respectively. Thus, piezoelectric scattering is found to be an important scattering source for real strained QW's with a well width $L\gtrsim 50$ Å and predominant over surface roughness scattering with $L\gtrsim 100$ Å as quoted before.

The dependence of the piezoelectric scattering-limited mobility μ_{PE} on the well thickness L, showing up in Fig. 4, is governed by the following factors. First, in the lowest subband the majority of electrons are located at the center of the well. Consequently, when increasing L the distance between the electron system and the interface is increased, thus elevating the mobility μ_{PE} (and also μ_{SR}). Second, an increase of L leads obviously to a corresponding increase of the total number of piezoelectric charges present in the well, which act on the 2D motion of confined carriers, thus reducing the mobility μ_{PE}. In a narrow well, this overwhelms the first effect, leading to an overall decrease of μ_{PE}. However, as indicated in Refs. 10 and 11, the piezoelectric charges are located mainly in a near-surface region of a few correlation length with a density decaying rather rapidly far from the interface plane. Therefore, with a subsequent increase of L the total number of piezoelectric charges remains almost unchanged and the first effect is predominant, leading to an overall increase of μ_{PE}.

B. Comparison with experiments on strained InGaAs-based quantum well

We are now trying to apply the above-developed theory to explain some experimental findings about the low-temperature mobility of electrons in lattice-mismatched $In_xGa_{1-x}As$-based QW's.

The mobility in a QW made from $In_{0.2}Ga_{0.8}As/GaAs$ with a well width $L=120$ Å and a sheet electron density $n_s=1.2\times10^{12}$ cm^{-2} were reported in Ref. 6 to be $\mu^{(1)}_{expt}=3\times10^4$ cm^2/Vs. The data for a QW from $In_{0.15}Ga_{0.85}As/Al_{0.23}Ga_{0.77}As$ with $L=130$ Å and $n_s=1.5\times10^{12}$ cm^{-2} were reported in Ref. 7 to be much higher: $\mu^{(2)}_{expt}=7.3\times10^4$ cm^2/Vs.

It should be noted that the samples in question show the experimentally observed mobilities much smaller than those expected from the existing theories. Moreover, they exhibit a large difference in the mobility, viz. with a ratio of about 240%, although the differences in their structure and the In content are small (only 5%). These cannot be understood, starting from the so far-known scattering mechanisms. Indeed, it was pointed out[6] that for the $In_{0.2}Ga_{0.8}As/GaAs$ QW, scattering by ionized dopants would yield a mobility much larger than the observed: $\mu_{ID}=3\times10^5$ cm^2/Vs. Also, the mobility dominated by alloy disorder was estimated[5] to be large: $\mu_{AD}=2.4\times10^5$ cm^2/Vs.

Therefore, to explain the low measured mobility of electrons in the above samples, Lyo and Fritz[6] had to propose another scattering source which stems from strain fluctuations due to a random distribution of In atoms. With a best choice of the deformation-potential constants, their theory was found to be able to reproduce the experimental data for the $In_{0.15}Ga_{0.85}As/Al_{0.23}Ga_{0.77}As$ system,[7] but not for the $In_{0.2}Ga_{0.8}As/GaAs$ one.[6] Hence, these authors had to invoke an idea of clustering of In atoms into one unit in the strained $In_xGa_{1-x}As$ layer. They claimed the average cluster size for the $In_{0.2}Ga_{0.8}As$ and $In_{0.15}Ga_{0.85}As$ layers to be 3 and 1, respectively, assuming its dependence on the growth conditions. The clustering effect was actually confirmed by a recent experiment,[41] where clusters containing $2-3$ In atoms were observed by using a cross-sectional scanning tunneling microscope in combination with its spectroscopic capability.

Nevertheless, the theory due to Lyo and Fritz with inclusion of In clustering turns out to be, to some extent, still unsatisfactory. Indeed, it was reported in Ref. 41 that in the $In_{0.2}Ga_{0.8}As$ layer, a large majority of the clusters (up to about 80%) contain two In atoms, whereas only about 15% contain three In atoms as claimed by the Lyo-Fritz theory. Thus, this theory is able to provide only a crude description of the result in Ref. 6. Furthermore, basing on the experimental observation that the In clustering occurs simply in an $In_xGa_{1-x}As$ layer under strain and preferentially along the growth direction, Zheng and co-workers[41] have shown that local strain dominates the formation of clusters in the layer. This means that we may ignore the other clustering mechanisms such as random clustering, chemical, and correlation effects. Also, the cluster size may be dependent on the growth conditions, but primarily fixed by the strain in the layer. Therefore, the difference in cluster size between the $In_{0.2}Ga_{0.8}As$ and $In_{0.15}Ga_{0.85}As$ layers must not be so large as claimed in Ref. 6, since their difference in lattice mismatch, i.e., in strain, is small. Thus, the large difference in the mobility of the systems reported in Refs. 6 and 7, despite a small difference in their structure and the In content, might still remain as a challenging problem in the theory of electron mobility for strained $In_xGa_{1-x}As$ QW's.

Starting from the foregoing theory, we suggest that the observed difference in the mobility is due mainly to a roughness-induced random piezoelectric field. Accordingly, we have evaluated the overall mobility of the systems in question, μ_{tot}, which is to be limited by both piezoelectric and surface roughness scattering, employing Eq. (17). The results thus obtained are presented in Figs. 5 and 6 as a function of the correlation length Λ. In Fig. 5 this is plotted for the $In_{0.2}Ga_{0.8}As/GaAs$ sample with a lattice mismatch $\epsilon_\parallel=-1.48\%$, while in Fig. 6 for the $In_{0.15}Ga_{0.85}As/Al_{0.23}Ga_{0.77}As$ system with $\epsilon_\parallel=-1.11\%$.

In the calculation of the total mobility in strained InGaAs-based QW's we have included the clustering effect arising from strain. Zheng and co-workers[41] have indicated that In clustering and segregation are the main reasons for the roughness in strained $In_xGa_{1-x}As$ QW's. Therefore, these exert a crucial influence on the interface properties. Within a continuum model for the interface of a semiconductor heterostructure, the effect may be taken adequately into account in terms of the parameters characteristic of the interface profile, in particular, the roughness amplitude. Indeed, Xie and co-workers[42] have shown with the use of atomic force microscopy that the roughness amplitude is elevated when increasing the strain, i.e., the lattice mismatch. The experimen-

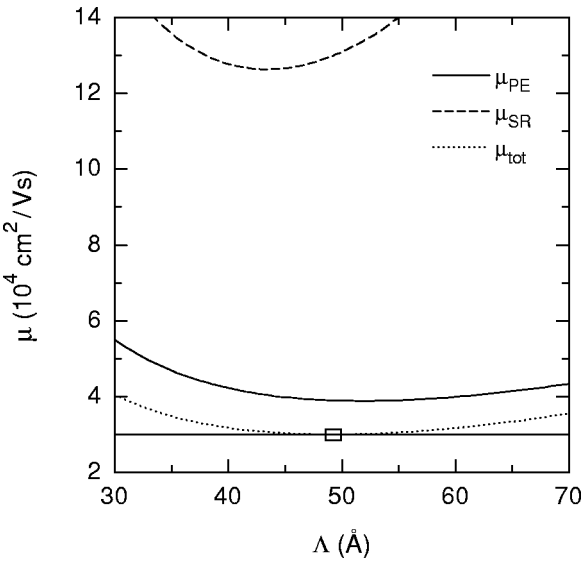

FIG. 5. Mobilities calculated for the QW in Ref. 6, made from $In_{0.2}Ga_{0.8}As/GaAs$ with a well width $L=120$ Å and an electron density $n_s=1.2\times10^{12}$ cm^{-2} vs correlation length Λ for a roughness amplitude $\Delta=8.5$ Å. The solid, dashed, and dotted lines refer to μ_{PE}, μ_{SR}, and μ_{tot}, respectively. The experimental data $\mu^{(1)}_{expt}=3\times10^4$ cm^2/Vs are marked by a horizontal.

tal result illustrating this relation was reported in Refs. 42 and 43 for the case of strained $Si/Si_{1-x}Ge_x$ QW's, e.g., $\Delta=15.5$ Å for $x=0.2$.

It is well known[44,45] that the interfaces of a lattice-matched (unstrained) $In_xGa_{1-x}As$ QW, e.g., made from $In_{0.53}Ga_{0.47}As/InP$ are extremely flat, so that the roughness amplitude is very small ($\Delta<1$ Å), and surface roughness scattering was ignored in the mobility calculation.[5,46,47] Owing to In clustering and segregation, the interfaces of a strained $In_xGa_{1-x}As$-based QW become very rough, so that the roughness amplitude must be chosen much larger than the one for an unstrained $In_{0.53}Ga_{0.47}As/InP$ QW. Indeed, based on the experimental data of photoluminescence linewidths from a strained $In_{0.2}Ga_{0.8}As/GaAs$ surface QW, Dreybrodt and co-workers[48] have reported a roughness amplitude $\Delta=12$ Å. It turns out that the measured mobility reported in Ref. 6 may be exactly reproduced with $\Delta=8.5$ Å and $\Lambda=49$ Å, while the one in Ref. 7 with $\Delta=8.2$ Å and $\Lambda=45.2$ Å. The good quantitative agreement between our theory and the experimental data supplies an evidence for the importance of the clustering effect in strained $In_xGa_{1-x}As$ QW's. It is worth noting that the roughness amplitude in use is also larger than the one for other unstrained systems, e.g., $\Delta=3$ Å for GaAs/AlAs.[4]

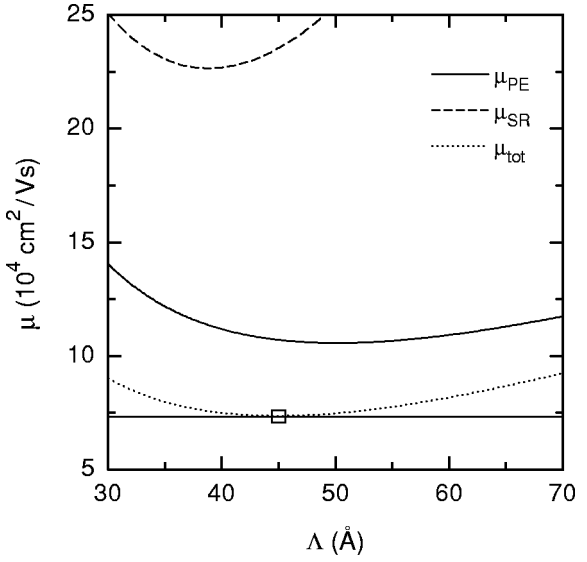

FIG. 6. Mobilities calculated for the QW in Ref. 7, made from $In_{0.15}Ga_{0.85}As/Al_{0.23}Ga_{0.77}As$ with a well width $L=130$ Å and an electron density $n_s=1.5\times10^{12}$ cm^{-2} vs correlation length Λ for a roughness amplitude $\Delta=8.2$ Å. The solid, dashed, and dotted lines refer to μ_{PE}, μ_{SR}, and μ_{tot}, respectively. The experimental data $\mu^{(2)}_{expt}=7.3\times10^4$ cm^2/Vs are marked by a horizontal.

In addition, an inspection of Figs. 5 and 6 indicates that piezoelectric scattering dominates, in fact, the electron mobilities under study. The larger mobility of the sample made from $In_{0.15}Ga_{0.85}As/Al_{0.23}Ga_{0.77}As$ is evidently seen to be connected with a larger well thickness, a higher electron density, and also a weaker strength of piezoelectric scattering. Indeed, the ratio of the autocorrelation function for piezoelectric scattering in this sample to that in the $In_{0.2}Ga_{0.8}As/GaAs$ system is found, according to Eq. (46), to be 0.79.

Next, we are examining the validity of the linear transport theory adopted in our mobility calculation for the samples studied in Refs. 6 and 7. The theoretical estimates are exact enough with no multiple scattering effect. Indeed, this was shown[5] to be noticeable only for a low electron density $n_s\lesssim1\times10^{11}$ cm^{-2}.

C. Further applications

To end this section, we will give a brief discussion on the possibility of applying our theory to understand transport in other lattice-mismatched semiconductor heterostructures.

First, we are concerned with the low-temperature mobility of holes in $Si/Si_{0.8}Ge_{0.2}$ heterostructures, where conduction takes place in the strained $Si_{0.8}Ge_{0.2}$ layer. It was pointed out[49–51] that the well-known scattering mechanisms are unable to account for their low measured hole mobility. Therefore, a special scattering source due to a high density of interface charges must be invoked. It was argued[51] that this is an intrinsic phenomenon not associated with unintentional doping of the alloy and might be piezoelectric in origin. Several experimental evidences for piezoelectricity of strained SiGe layers have recently been found.[51–55]

Following the above idea, we suggest that this might be random piezoelectric charges, which are generated as a result of the combination of both lattice-mismatch and surface-roughness effects in an actual strained $Si/Si_{0.8}Ge_{0.2}$ system. Indeed, piezoelectric charges which are generated in a strained heterostructure with ideal interfaces was demonstrated[25] to be nonrandom, and uniformly distributed on the interfaces. Therefore, their piezoelectric field is nonrandom and points along the growth direction. This implies that the piezoelectric charges created merely by a lattice-

mismatch effect can only modify the confining potential for the quantized motion. This also means that they present no scattering source in the in-plane motion of confined charge carriers, exerting no influence on their mobility.

Second, it is worth mentioning that in the last few years there has been great interest in strained nitride heterostructures, e.g., $In_xGa_{1-x}N/GaN$ and AlN/GaN QW's, in view of their high potential for fabrication of high frequency and high power electronic devices. The low-temperature mobility of electrons in, e.g., AlN/GaN systems was reported[56,57] to be quite low (7.2×10^2 cm^2/Vs at an electron density of 4.8×10^{12} cm^{-2}). We speculate that the random piezoelectric field drastically affects their electric properties since group-III nitrides have large piezoelectric constants.[58–60]

VI. SUMMARY

To summarize, in the present paper we have proved that in real lattice-mismatched QW's there always exist random fluctuations in the strain field. In the case of zinc-blende structure QW's, the strain variations can produce a large fluctuating density of piezoelectric charges even with a high symmetry growth axis, e.g., [001]. Their piezoelectric field arises as a combined effect from both lattice mismatch and surface roughness and is random in nature, whereas the conventional piezoelectric field in ideal QW's is only due to lattice mismatch and non-random.

The random piezoelectric field turns out to be a new important scattering mechanism for real zinc-blende structure QW's, especially those with a well width of the order of or greater than 50 Å. This is found to be predominant over surface roughness scattering when the well width is larger than about 100 Å. In combination with the latter, the former provides an accurate way to explain a large difference in electron mobility despite a small difference in In content observed in lattice-mismatched InGaAs-based QW's.

Scattering by a random piezoelectric field might be one of the principal processes limiting the low-temperature hole mobility measured in real strained Si/SiGe heterostructures. Moreover, it might be mandatory to take into account the impact of the random piezoelectric field in the interpretation of observable properties as well as the design and development of new strained nitride-based electronic devices.

ACKNOWLEDGMENTS

One of the authors (D.N.Q.) would like to thank Professor M. Saitoh for valuable discussion and generous hospitality during his stay at the Department of Physics, Graduate School of Science, Osaka University, Japan. He is deeply grateful to the Japan Society for the Promotion of Science for a fellowship, under which this work was done.

[1] T. Ando, A.B. Fowler, and F. Stern, Rev. Mod. Phys. **54**, 437 (1982).
[2] R.E. Prange and T.W. Nee, Phys. Rev. **168**, 779 (1968).
[3] A. Gold, Phys. Rev. B **35**, 723 (1987).
[4] H. Sakaki, T. Noda, K. Hirakawa, M. Tanaka, and T. Matsusue, Appl. Phys. Lett. **51**, 1934 (1987).
[5] A. Gold, Phys. Rev. B **38**, 10 798 (1988).
[6] S.K. Lyo and I.J. Fritz, Phys. Rev. B **46**, 7931 (1992).
[7] N. Pan, J. Carter, X.L. Zheng, H. Hendriks, C.H. Wu, and K.C. Hsieh, Appl. Phys. Lett. **58**, 71 (1991).
[8] D.J. Srolovitz, Acta Metall. **37**, 621 (1989).
[9] R.M. Feenstra and M.A. Lutz, J. Appl. Phys. **78**, 6091 (1995).
[10] D.N. Quang, V.N. Tuoc, N.H. Tung, and T.D. Huan, Phys. Rev. Lett. **89**, 077601 (2002).
[11] D.N. Quang, V.N. Tuoc, N.H. Tung, and T.D. Huan, Phys. Rev. B **68**, 153306 (2003).
[12] R.M. Feenstra, M.A. Lutz, F. Stern, K. Ismail, P.M. Mooney, F.K. LeGoues, C. Stanis, J.O. Chu, and B.S. Meyerson, J. Vac. Sci. Technol. B **13**, 1608 (1995).
[13] T. Ando, J. Phys. Soc. Jpn. **51**, 3893 (1982); **51**, 3900 (1982).
[14] Y. Okuyama and N. Tokuda, Phys. Rev. B **40**, 9744 (1989).
[15] K. Schmalz, I.N. Yassievich, E.J. Collart, and D.J. Gravesteijn, Phys. Rev. B **54**, 16 799 (1996).
[16] U. Penner, H. Rücker, and I.N. Yassievich, Semicond. Sci. Technol. **13**, 709 (1998).
[17] G. Traetta, G. Coli, and R. Cingolani, Phys. Rev. B **59**, 13 196 (1999).
[18] F.M.S. Lima, Q. Fanyao, O.A.C. Nunes, and A.L.A. Fonseca, Phys. Status Solidi B **225**, 43 (2001).
[19] A. Gold and W. Götze, Phys. Rev. B **33**, 2495 (1986).
[20] F. Stern and W.E. Howard, Phys. Rev. **163**, 816 (1967).
[21] B. Laikhtman and R.A. Kiehl, Phys. Rev. B **47**, 10 515 (1993).
[22] S. Das Sarma and B.A. Mason, Ann. Phys. (N.Y.) **163**, 78 (1985).
[23] M. Jonson, J. Phys. C: Solid State Phys. **9**, 3055 (1976).
[24] E. Anastassakis, J. Appl. Phys. **68**, 4561 (1990).
[25] D.L. Smith and C. Mailhiot, Rev. Mod. Phys. **62**, 173 (1990).
[26] In Ref. 10 the shear modulus G was incorrectly reported and should be equal to a fourth of G defined in this paper.
[27] M. Ilg, A. Heberle, and K.H. Ploog, Solid-State Electron. **37**, 739 (1994).
[28] M. Ilg, K.H. Ploog, and A. Trampert, Phys. Rev. B **50**, 17 111 (1994).
[29] J.P. Hirth and J. Lothe, *Theory of Dislocations* (Wiley, New York, 1982).
[30] A.D. Bykhovski, B.L. Gelmont, and M.S. Shur, J. Appl. Phys. **78**, 3691 (1995); **81**, 6332 (1997); Appl. Phys. Lett. **73**, 3577 (1998).
[31] M. Grundmann, O. Stier, and D. Bimberg, Phys. Rev. B **52**, 11 969 (1995).
[32] D.A. Faux, J.R. Downes, and E.P. O'Reilly, J. Appl. Phys. **82**, 3754 (1997).
[33] J.H. Davies, J. Appl. Phys. **84**, 1358 (1998).
[34] J.F. Nye, *Physical Properties of Crystals* (Oxford University Press, Oxford, 1964).
[35] E. Anastassakis, Phys. Rev. B **46**, 4744 (1992).
[36] B.K. Ridley, *Quantum Processes in Semiconductors*, 2nd ed. (Clarendon, Oxford, 1988).

[37] M. Neuberger, *Handbook of Electronic Materials*, Vol. 2 (IFI/Plenum, New York, 1971).
[38] C.G. Van de Walle, Phys. Rev. B **39**, 1871 (1989).
[39] P. Harrison, *Quantum Wells, Wires, and Dots: Theoretical and Computational Physics* (Wiley, New York, 2000).
[40] Al.L. Efros, C. Wetzel, and J.M. Worlock, Phys. Rev. B **52**, 8384 (1995).
[41] J.F. Zheng, J.D. Walker, M.B. Salmeron, and E.R. Weber, Phys. Rev. Lett. **72**, 2414 (1994).
[42] Y.H. Xie, G.H. Gilmer, C. Roland, P.J. Silverman, S.K. Buratto, J.Y. Cheng, E.A. Fitzgerald, A.R. Kortan, S. Schuppler, M.A. Marcus, and P.H. Citrin, Phys. Rev. Lett. **73**, 3006 (1994).
[43] T.E. Whall and E.H.C. Parker, J. Phys. D **31**, 1397 (1998); Thin Solid Films **368**, 297 (2000).
[44] M. Takikawa, J. Komeno, and M. Ozeki, Appl. Phys. Lett. **43**, 280 (1983).
[45] W.T. Tsang and E.F. Schubert, Appl. Phys. Lett. **49**, 220 (1986).
[46] D.A. Anderson, S.J. Bass, M.J. Kane, and L.L. Taylor, Appl. Phys. Lett. **49**, 1360 (1986).
[47] M.J. Kane, D.A. Anderson, L.L. Taylor, and S.J. Bass, J. Appl. Phys. **60**, 657 (1986).
[48] J. Dreybrodt, A. Forchel, and J.P. Reithmaier, Phys. Rev. B **48**, 14 741 (1993).
[49] C.J. Emeleus, T.E. Whall, D.W. Smith, R.A. Kubiak, E.H.C. Parker, and M.J. Kearney, J. Appl. Phys. **73**, 3852 (1993).
[50] R.J.P. Lander, M.J. Kearney, A.I. Horrell, E.H.C. Parker, P.J. Phillips, and T.E. Whall, Semicond. Sci. Technol. **12**, 1064 (1997).
[51] M.A. Sadeghzadeh, A.I. Horrell, O.A. Mironov, E.H.C. Parker, T.E. Whall, and M.J. Kearney, Appl. Phys. Lett. **76**, 2568 (2000).
[52] Y.H. Xie, R. People, J.C. Bean, and K.W. Wecht, Appl. Phys. Lett. **49**, 283 (1986).
[53] Y.H. Xie, R. People, J.C. Bean, and K.W. Wecht, J. Vac. Sci. Technol. B **5**, 744 (1987).
[54] O.A. Mironov, V.I. Khizhny, G. Braithwaite, E.H.C. Parker, P.J. Phillips, T.E. Whall, and V.P. Gnezdilov, J. Cryst. Growth **157**, 382 (1995).
[55] V.I. Khizhny, O.A. Mironov, E.H.C. Parker, P.J. Phillips, T.E. Whall, and M.J. Kearney, Appl. Phys. Lett. **69**, 960 (1996).
[56] S.C. Binari, K. Doverspike, G. Kelner, H.B. Dietrich, and A.E. Wickenden, Solid-State Electron. **41**, 177 (1997).
[57] I.P. Smorchkova, S. Keller, S. Heikman, C.R. Elsass, B. Heying, P. Fini, J.S. Speck, and U.K. Mishra, Appl. Phys. Lett. **77**, 3998 (2000).
[58] T. Takeuchi, S. Sota, M. Katsuragawa, M. Komori, H. Takeuchi, H. Amano, and I. Akasaki, Jpn. J. Appl. Phys., Part 2 **36**, L382 (1997).
[59] T. Takeuchi, C. Wetzel, S. Yamaguchi, H. Sakai, H. Amano, I. Akasaki, Y. Kaneko, S. Nakagawa, Y. Yamaoka, and N. Yamada, Appl. Phys. Lett. **73**, 1691 (1998).
[60] F. Bernardini, V. Fiorentini, and D. Vanderbilt, Phys. Rev. B **56**, R10 024 (1997).